



A modelling approach combining swat with Gis-based DRASTIC techniques to assess aquifer vulnerability evolution in highly anthropised aquifers

Francisco J. Segura-Méndez¹ · Julio Pérez-Sánchez² · Adrián López-Ballesteros¹ · Javier Senent-Aparicio¹

Received: 28 August 2024 / Accepted: 26 October 2024 / Published online: 9 November 2024
© The Author(s), under exclusive licence to Springer-Verlag GmbH Germany, part of Springer Nature 2024

Abstract

Groundwater resources are vital for human development, particularly in arid and semi-arid regions with limited water availability. This study examines the evolution of aquifer vulnerability in the Miranda basin by addressing the critical interaction between land use and water quality amidst increasing pressures on water resources, with a focus on the impact of historical land use changes and agricultural practices on groundwater quality in the Campo de Cartagena aquifer, which drains into the degraded Mar Menor coastal lagoon in southern Spain. To evaluate aquifer vulnerability, this research employs the DRASTIC vulnerability assessment method, which is based on seven hydrogeological parameters. This theoretical framework allows for a comprehensive analysis of the interactions between land use changes, water management, and aquifer health, which deepens the understanding of the factors driving vulnerability over time. A key component of the methodology is the use of the Soil and Water Assessment Tool (SWAT) to estimate aquifer recharge and generate reliable maps that depict this essential parameter. The study reveals significant results through an extensive analysis of vulnerability changes over the past 70 years, which shows that high vulnerability areas have increased from 11%, prior to the Tagus-Segura water transfer in 1979, to 53% today. In contrast, low and moderate vulnerability areas have decreased by 15% and 28%, respectively. This shift is primarily attributed to intensified agricultural practices, which lead to enhanced aquifer recharge and elevated piezometric levels, which increase contamination risks, as demonstrated by the severe eutrophication observed in the Mar Menor. Moreover, the accuracy of the vulnerability maps is validated by comparing them with observed nitrate concentrations in groundwater, which reveals a strong correlation ($R^2 = 0.86$). The methodology provides essential insights for policymakers and supports the implementation of land use restrictions to mitigate groundwater contamination risks. The findings ultimately underscore the necessity for integrated water management strategies that balance agricultural productivity with ecological sustainability in water-scarce environments.

Keywords Aquifer vulnerability assessment · Landuse changes · DRASTIC · SWAT · GIS · Water resources management

✉ Francisco J. Segura-Méndez
fjsegura@ucam.edu

Julio Pérez-Sánchez
julio.sanchez@ulpgc.es

Adrián López-Ballesteros
alopez6@ucam.edu

¹ Department of Civil Engineering, Catholic University of San Antonio, Campus de Los Jeronimos s/n, Guadalupe, Murcia 30107, Spain

² Department of Civil Engineering, Universidad de Las Palmas de Gran Canaria, Campus de Tafira, Las Palmas de Gran Canaria 35017, Spain

Introduction

Anthropogenic activities such as urbanisation, industry and farming are considered the main drivers of the transformation of the Earth's biosphere (Niemelä et al. 2000; Ellis 2015; Singh et al. 2021). Human societies are responsible for the most contemporary changes in current environments (Jansen and Gregorio 2002; Tuomainen and Candin 2011). Numerous studies have highlighted how mankind has caused significant alterations worldwide in global warming (Cook et al. 2016), biodiversity loss (Hautier et al. 2015), soil erosion (Issaka and Ashraf 2017), eutrophication

(Chuai et al. 2012) and fire regimes (Bowman et al. 2011). Consequently, water resources are not an exception, human pressures and climate change result in a large geographical and temporal variability of both surface water and groundwater quality and quantity (Ghaleni and Ebrahimi 2015).

Water stress and scarcity are becoming increasingly important for many countries (du Plessis 2019) due to population growth, urbanisation, irrigation demands, pollution and climate change, this affects over 2 billion people in the world (Phok et al. 2021). In this regard, within the 2030 Agenda for Sustainable Development of the United Nations, Goal 6 focuses on ensuring the universal availability of drinking water and sanitation, as well as its sustainable development and management. Indeed, target 6.3 addresses improving water quality by 2030 by reducing contamination, eliminating wastewater discharge, reducing chemical emissions and hazardous materials, halving untreated raw sewage, and strongly increasing recycling and reuse. Indicator 6.3.2. outlines the proportion of bodies of water with good ambient water quality, which is measured by various sub-indicators, such as 6.3.2.3. which assesses groundwater bodies overall status. The monitoring, control and supervision of groundwater quality is crucial for meeting the proposed objectives (Pacheco et al. 2018; Lapworth et al. 2022) point note that groundwater contamination risk models must be integrated in watershed scale management to assess aquifer vulnerability.

Groundwater has been a vital resource for humankind throughout history, representing the greatest freshwater reservoir on Earth in living areas. On a global level, over 97% of accessible water in the world is provided by aquifers from which half of drinking and irrigation water comes from them (Jakeman et al. 2016). Furthermore, the role of aquifers in environmental issues is also noteworthy, are a key factor in base flow to rivers and riverbanks and floodplains moisture. In recent decades, the use of groundwater increased substantially, particularly in irrigation in arid and semiarid regions (Moench 2003; Schmid et al. 2005; Custodio Gimena et al. 2016; Domingo-Pinillos et al. 2018; Senarathne et al. 2021). Aquifer overexploitation has led to critical depletions in water tables (Bhattarai et al. 2021), reductions (even disappearance) in river and spring flow rates (Souza et al. 2022), negative effects in wetlands and riparian ecosystems (Li et al. 2021), degradation in water quality (Dhaouadi et al. 2021; Sarah et al. 2021; Ouarekh et al. 2021) and sea intrusion in coastal aquifers (Hajji et al. 2022; Idowu et al. 2022).

In Mediterranean regions, semi-arid climate, seasonal droughts and high-variability rainfall have led to a great exploitation of groundwater resources over millennia, but their water supplies have been considerably reduced in the last 50 years (Cudennec et al. 2007), particularly to satisfy

agriculture demands and tourism in coastal cities (Iglesias et al. 2007). A clear example of anthropisation in the western Mediterranean is the multilayer aquifer at Campo de Cartagena (CC) (Senent-Aparicio et al. 2015), region of great economic and touristic value located in southern Spain. The main sector is agriculture, which is highly influenced by the scarcity of water problems in the area. Due to the absence of natural permanent surface water, groundwater, the Tajo-Segura water transfer, and the reuse of wastewaters are the main resources to meet water demands (Rupérez-Moreno et al. 2017). The implementation of the water transfer in 1979 caused a radical change in irrigable zones in both land use and environmental situation (Senent-Aparicio et al. 2021). There was a significant increase in irrigated intensive farming marked-orientated crops such as citrus trees, fruit trees and vegetables versus previous traditional agriculture based on un-irrigated fruit-bearing crops (Ibarra Marinas et al. 2017). Concerning the aquifer, the deficit caused by the large number of water withdrawals in the pre-water transfer period was replaced by positive balance in the post-transfer period, due to reduction of around 50% in groundwater abstraction and the increase of infiltration from the irrigation surpluses (Domingo-Pinillos et al. 2018).

The CC aquifer is a clear example of significant spatial and temporal variations in groundwater systems, with direct implications in both water quality and quantity. Water resources policy at all levels of government is required to analyse the evolution of the vulnerability of groundwater to provide the tools to plan appropriate measures in the sustainable utilisation of water resources as well as in land-use regulation and growth management. Indeed, Pisciotta et al. (2015) address the vulnerability in aquifers to all the factors depending on space and time that can contribute modifying groundwater quality. In essence, the assessment of the vulnerability of an aquifer relies on contaminant agents and hydrologic and hydrogeologic processes (Bera et al. 2021). Vulnerability methods can be classified into four categories: overlay and index-based methods, process-based simulation models, statistical methods, and hybrid methods (Taghavi et al. 2022).

Amongst the former, the most popular in groundwater vulnerability research are DRASTIC (Ahada and Suthar 2018; Nazzal et al. 2019; Oke 2020; Shah et al. 2021; Ahmed et al. 2022), GALDIT (Mahrez et al. 2018; Amarni et al. 2020; Idowu et al. 2022), SINTACS (Noori et al. 2019; Jahromi et al. 2021; Ikenna et al. 2021), the susceptibility index (Ncibi et al. 2020; Ameer et al. 2021), and GOD (Ekanem 2022).

Previous studies have compared the above indices (Ourahi et al. 2024a, b) in various aquifers around the world and generally demonstrated the superiority of DRASTIC over all others. Quantitative methods or process-based approaches

are based on water and pollutant transport models and, use deterministic physical and chemical equations to represent the process of pollutant transport and transformation (Geng et al. 2023). The complexity of the models varies depending on the required datasets and the equations relating them (Machiwal et al. 2018). Within this category, the most commonly used models to simulate water flow and solute transport can be classified into hydraulic models, such as SWAP (Claus Henn et al. 2018) and MODFLOW (Eslamian et al. 2023); multicomponent geochemical models, such as PHREEQC (Abdelshafy et al. 2019) and MINTEQ (Lai et al. 2019); and coupled models for water flow, solute transport, and chemical reactions (Testoni et al. 2017). Statistical methods offer an effective option for assessing aquifer vulnerability when the relationship between groundwater quality and environmental information (Fannakh and Farsang 2022), such as hydrogeological data, soil characteristics, and land use, is susceptible. The most common statistical techniques for assessing vulnerability include logistic regression (Jang 2022), multiple linear regression (Busico et al. 2020), and artificial intelligence models (Jafarzadeh et al. 2024), with the latter being used in predicting vulnerability in aquifers.

Despite the numerous existing techniques for the assessment of vulnerability in aquifers, index-based methods, which are qualitative in nature, continue to be the most widely used models (Rezaei et al. 2013), primarily because they are integrated with geographic information systems (GIS), which allows users to interpret the results more easily (Ourarhi et al. 2024a). Over time, the DRASTIC method has proven to be an effective and reliable tool for protecting, managing, and monitoring groundwater resources against surface pollution (Ourarhi et al. 2024c). Nonetheless, in the last decade, numerous studies have also proposed several modifications to this index. For example, Ourarhi (Ourarhi et al. 2024c) integrated the DRASTIC, RIVA (Tziritis et al. 2021), and analytic hierarchy process (AHP) (Saaty 1988) techniques to enhance and streamline the assessment of groundwater vulnerability in Moroccan agricultural regions. Likewise, the AHP and variable weight model (VWM) methods, combined with DRASTIC, were employed by Yu (Yu et al. 2013) to optimise the weighting of parameters in a vulnerability assessment in central China. Furthermore, recent review studies on groundwater vulnerability assessment (Taghavi et al. 2022) highlight the scarcity of studies based on hybrid approaches. The novelty and usefulness of the methodology employed in this work, combining index and process based methods, is thus particularly interesting in highly anthropised areas. In fact, the use of the Soil and Water Assessment Tool (SWAT) to estimate aquifer recharge ensures the generation of reliable results

representing this essential parameter and its influence on the calculated index.

This paper analyses the temporal evolution of the vulnerability of a semi-arid aquifer starting before the Tagus-Segura water transfer came into operation until the present day in the CC basin due to the diverse anthropisation processes in the area (aquifer overexploitation, water transfer, increase of irrigated agriculture and infiltration), using a GIS-based DRASTIC model. Furthermore, to provide more accurate R values in the DRASTIC method, as suggested by several research studies (Oni et al. 2017; Abunada et al. 2021), the semi-distributed soil SWAT model (Arnold et al. 1998) used to assess aquifer recharge.

Study area

The study area lie in the southeast of the Iberian Peninsula in the Segura River basin (Fig. 1). The Miranda watershed covers around 100 km² and is confined between 1°5' W to 0°51' longitude and 37°43' to 37°37' N latitude. Altitudes vary from 156 to 0 m above mean sea level (MAMSL), with an average of 20 m MAMSL. The study area is characterised by a long, flat plain defined by a little small southeast slope that is encircled by mountainous elevations in all its contours, except for the coastline area.

The Miranda watershed has a semi-arid Mediterranean climate, characterised by tempered winters and warm summers with a maximum of 40°C (August) and minimum of 10°C (January). The mean annual temperature and precipitation are around 17°C and 300 mm, respectively (1951–2019 period). There is a highly uneven distribution of rainfall over the year. Convective rain events are common in autumn and winter and may produce severe storms reaching over 100 mm in 24 h. There are no permanently flowing rivers in the studied watershed; only ephemeral watercourses drain this area of 99.16 km², with a maximum length of 18.89 km draining completely to the Mar Menor coastal lagoon.

The Miranda aquifer is part of a complex hydrogeological unit located in the large inland depressions of the Betic Cordilleras. It is dominated by a powerful Neogene fill and contains calcareous and detrital intercalations from the Miocene to the Quaternary, which form different aquifer levels. These diverse hydrogeological formations are composed of sand, silt, clay, conglomerate, caliche, and sandstone (Quaternary), sandstone (Pliocene), limestone (Messinian), sandy limestone and conglomerate (Tortonian) and marble from the Triassic bedrock (Baudron et al. 2014).

The exploitation of natural resources and changes in consumer habits, commodities, and processes in the area have resulted in an exponential rate of anthropogenic activities in

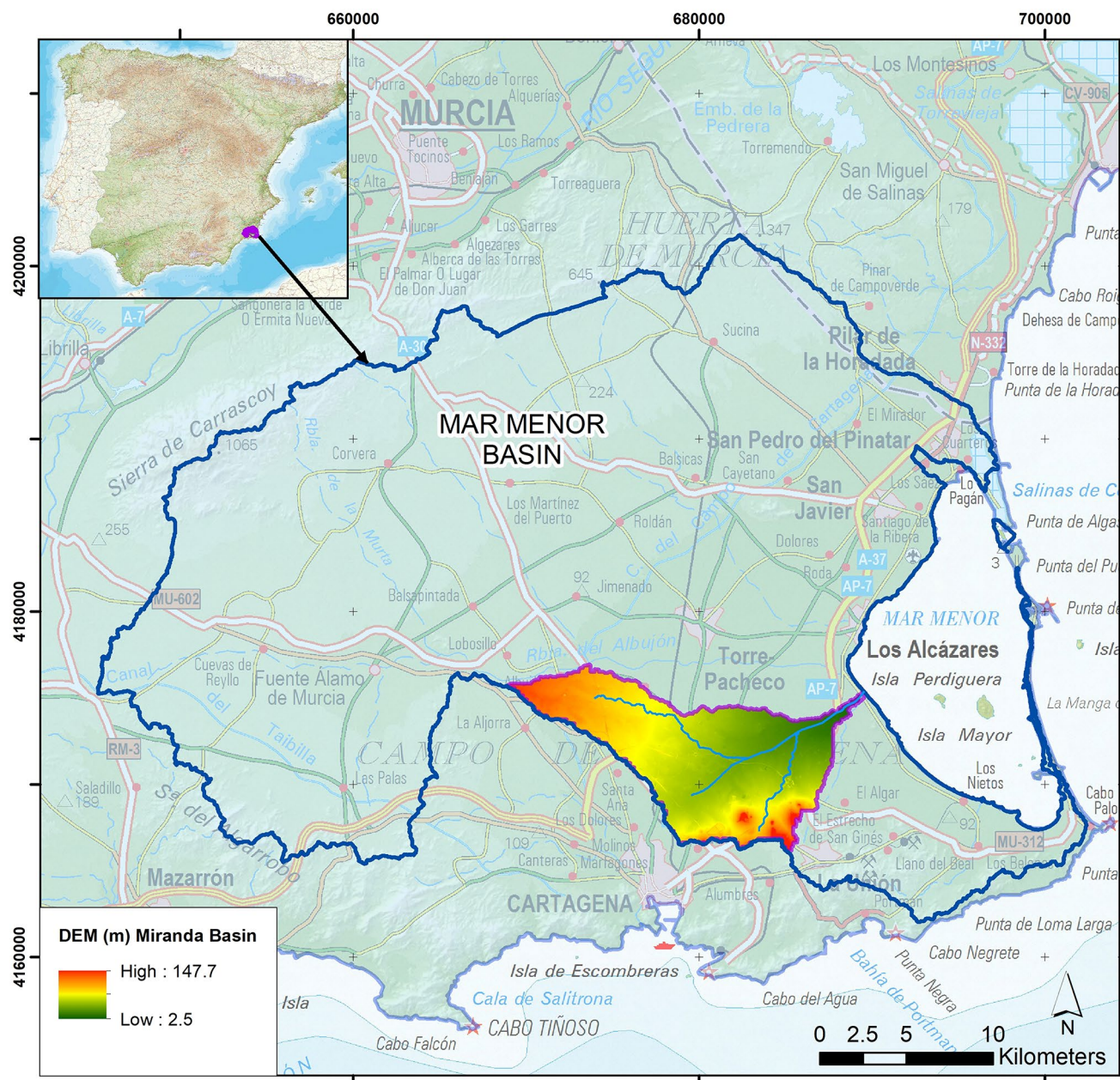


Fig. 1 Location of the Segura river basin and Miranda watershed, including topographic and river stream features

the last 60 years (Albuquerque et al. 2013). Agro-industrial activity has been and remains the most important economic sector in the Miranda basin, with crops covering more than third of the total surface area. In addition, none of the numerous small scattered urban centres exceeds 5,000 inhabitants across the studied area.

Materials and methods

In the present study, a GIS-based DRASTIC method has been used to evaluate the evolution of the vulnerability to pollution in the Miranda watershed aquifer over the past 70 years, by assessing the DRASTIC Vulnerability Index (DVI) distribution in the area starting from the Tagus-Segura water transfer came into operation until the present day with cell size of 1 km x 1 km. Based on the scarce availability of information, three time frames have been established to analyse the influence of agricultural expansion derived from the Tagus-Segura water transfer: (1) the 1950s, when the

Table 1 Data sources related to hydrogeological parameters

Data	Description	Source
Depth to Water (D)	Piezometric data	Database of Geological Survey of Spain (IGME)
Aquifer type (A); Soil type (S)	Geological map of Spain and Portugal	Geological Survey of Spain (IGME). 1:1,000,000
Impact of vadose zone (I)	lithostratigraphic map	Geological Survey of Spain (IGME). 1:200,000
Hydraulic conductivity (C)	Hydraulic conductivity raster	1 × 1 km of spatial resolution (Ferrer-Julia et al. 2021)

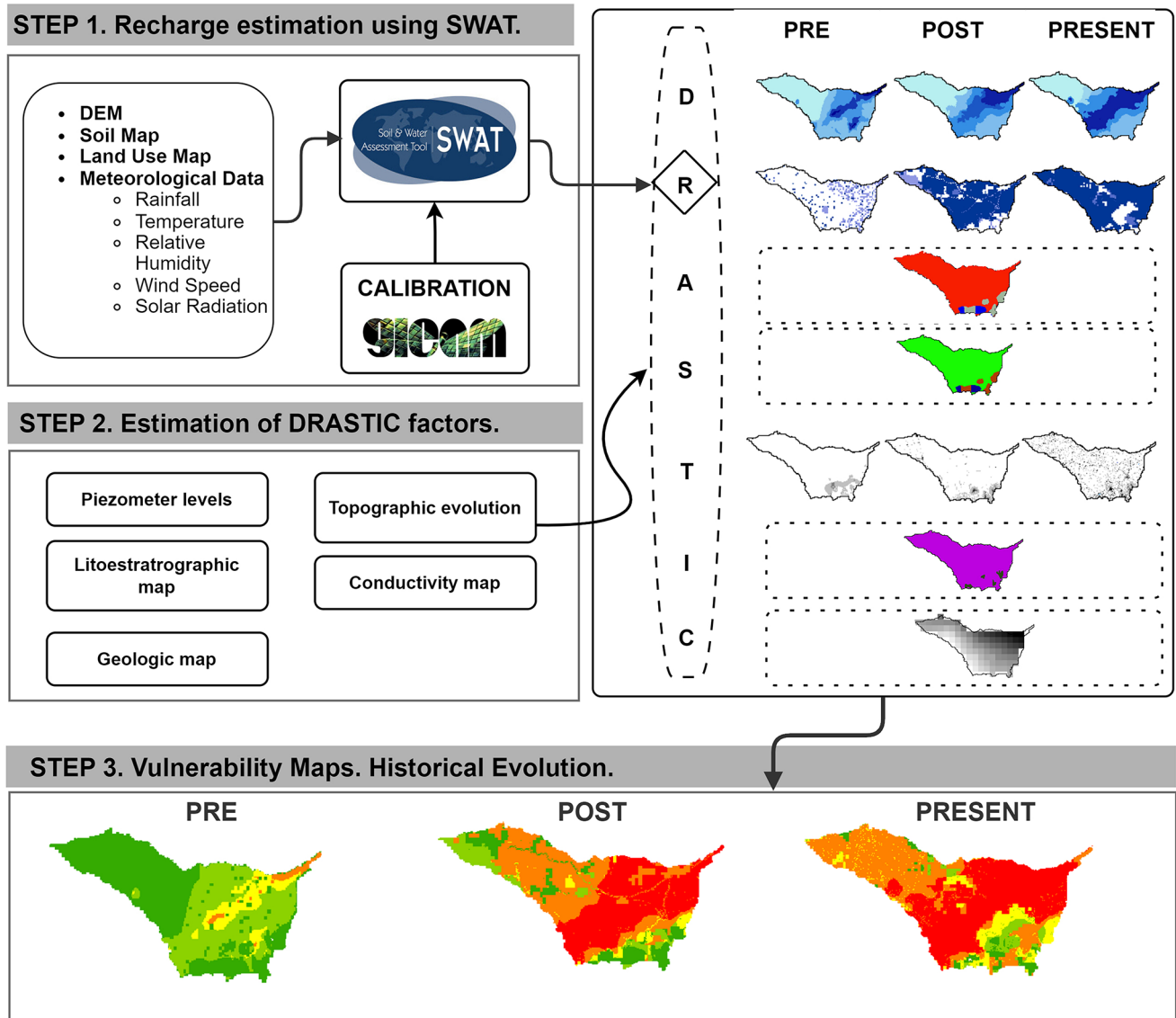


Fig. 2 Methodological flowchart

Tagus-Segura water transfer had not yet come into operation (PRE); (2) the 1990s, when agricultural expansion derived from water from the Tagus reached its peak (POST) and (3) the present time, when agricultural expansion is stabilised (PRESENT). The DRASTIC method (Aller and Thornhill 1987) is the most commonly used (Ncibi et al. 2020) due to its compatibility with a wide variety of aquifers (Asadi et al. 2016). The theoretical framework supporting the DRASTIC method is the rate from 1 (minimum vulnerability) to

10 (maximum vulnerability) according to the characteristics and behaviour of the seven environmental parameters controlling the groundwater pollution within the DRASTIC acronym: depth to groundwater (D), net recharge (R), aquifer type (A), soil type (S), topography (T), impact of the vadose zone (I) and conductivity of the aquifer (C) (Kwon et al. 2022) (Table 1).

The methodological approach followed in this work (Fig. 2) comprises three main steps: (1) the estimation of the

recharge factor based on a calibrated SWAT model (using satellite evapotranspiration data), (2) calculation of the other factors of the DRASTIC method based on available information, and (3) mapping of the historical evolution of aquifer vulnerability.

Depth to water (D)

D considers the depth of the piezometric level in the case of a free aquifer or the aquifer celling for a confined one; is a crucial component in determining the vulnerability to contamination in aquifers. The shallower the water table is, the faster contamination reaches groundwater. Since the beginning of the 20th century, the Geological Survey of Spain (IGME) has conducted numerous groundwater studies that provide information on piezometric data in CC. As such, D has been obtained from information provided by IGME for the various time periods (PRE, POST, and PRESENT).

Net recharge (R)

R is the primary means to transport contaminants from the vadose zone to the saturated zone. It mainly depends on soil permeability, land use, rainfall, and slope of terrain (Abunada et al. 2021). Various studies have analysed the components of parametric methods, including the DRASTIC model, and determined that aquifer recharge and depth are dynamic parameters, unlike the other variables, where they are regarded as static and remain unaffected by changes or surface pressure (Banerjee et al. 2023). For example, Ourarhi (Ourarhi et al. 2024b, d) combined the Groundwater Confinement Type, Hydraulic Conductivity, Vadose Zone Impact, Topography, and Dynamic Factor (GCITF), along with the DRASTIC method, in a Moroccan aquifer to achieve a more comprehensive analysis of dynamic anthropogenic pressure on the degree of vulnerability. The semi-distributed and physically based hydrological SWAT model (Arnold et al. 1998) was used at this stage for the various analysis periods. The catchment is divided into sub-basins that are further subdivided into hydrologic response units (HRUs), characterised by unique combinations of land use, soil and topographic characteristics. The water processes are simulated at individual HRUs, whose outputs are summed up and routed through the stream network. The hydrologic cycle is modelled at HRU level according to Eq. 1.

$$SW_t = SW_0 + \sum (R - Q_s - ET - W_{seep} - Q_{gw}) \quad (1)$$

where SW_t is the final soil water content (mm), SW_0 , the initial water content on day i (mm), R the precipitation on day i (mm), Q_s the surface runoff on day i (mm), ET the evapotranspiration on day i (mm), W_{seep} the amount of water entering the vadose zone on day i (mm) and Q_{gw} the return flow on day i (mm). Neitsch (Neitsch et al. 2011) provide a thorough description of all the parameters of the SWAT model.

2 shows the input data used in the present study for the SWAT model in the Miranda basin. The physical watershed characteristics were obtained using the 25-m spatial resolution DEM from the Spain National Geographic Institute (IGN). A map of crops and land uses in Spain for the 2000–2009 period was used to obtain the various landuses with the exception of 1960. This was done analysing black and white orthophotos from the 1956–1957 U.S. flight in the Segura Basin (CHS 2022). The land uses were classified according to the maximum likelihood algorithm (ML), under which probability density functions are built for each class based on the training data's spectral value (Hagner and Reese 2007). The process was performed by the Supervised Classification Plugin of QGIS (Congedo 2021). The soil physical parameters were obtained from the Harmonized World Soil Database (HWSD), which contains the soil properties information required for SWAT model, such as bulk density, soil depth, etc. Daily climate data from the Peninsular Spain Weather Dataset developed by Senent-Aparicio (Senent-Aparicio et al. 2021) were used as input in the SWAT model. A modified Soil Conservation Service (SCS) curve number and the Hargreaves methods were used to estimate surface runoff and potential evapotranspiration values, respectively (Table 2).

The model was set up for the 2000–2019 period, after which it was assessed for the three studied time frames (PRE, POST, and PRESENT). Three years (2000–2002) of warming-up were considered before the calibration and validation stages in the 2003–2012 and 2013–2019 periods, respectively. The soil evaporation compensation factor (ESCO), initial SCS runoff curve number (CN2), the plant update compensation factor (EPCO), the soil available water content (SOL_AWC), depth of soil layer (SOL_Z) and deep aquifer percolation fraction (RCHRG_DP) were determined as the most sensitive factors in the SWAT model. Actual evapotranspiration (AET) data obtained from the last version of the remote sensing dataset Global Land

Table 2 List of input datasets used for SWAT model setup

Data	Description	Source
DEM	25 m x 25 m resolution	Spanish National Geographic Institute (IGN)
Land use map	Vector database	Corine Land Cover (2000)
Soil map	1 km x 1 km resolution	Harmonized World Soil Map (HWSD)
Climate data	5 km x 5 km resolution	Spanish National Meteorological Agency (AEMET)

Evaporation Amsterdam Model (GLEAM) (Miralles et al. 2011) was used for calibration and validation processes (López-Ballesteros et al. 2019), by comparing the satellite-derived AET data with SWAT-simulated values. The Kling–Gupta efficiency index (KGE) (Eq. 2) was used to automate the calibration process (Gupta et al. 2009). The parameter ranges were changed after the first iteration of 1000 simulations, which were separated into two iterations of 500 runs each. The calibration and validation processes and global sensitivity analysis were conducted using the Sequential Uncertainty Fitting procedure (SUFI-2). The performance of the SWAT model was assessed using the coefficient of determination (R2) (Eq. 3), the percent bias (PBIAS) (Eq. 4) and Nash–Sutcliffe efficiency (NSE) (Eq. 5).

$$KGE = 1 - \sqrt{(\alpha - 1)^2 + (\beta - 1)^2 + (\gamma - 1)^2} \tag{2}$$

where α , β and γ are the Pearson correlation coefficient, fraction of standard deviation and the average between the observed and simulated AET data, respectively. KGE may vary between from $-\infty$ to 1, with 1 being the optimal value.

$$R^2 = \frac{\sum_{i=1}^n (AET_{obs,i} - \overline{AET_{obs}})(AET_{sim,i} - \overline{AET_{sim}})}{\sqrt{\sum_{i=1}^n (AET_{obs,i} - \overline{AET_{obs}})^2} \sqrt{\sum_{i=1}^n (AET_{sim,i} - \overline{AET_{sim}})^2}} \tag{3}$$

$$PBIAS = \frac{\sum_{i=1}^n (AET_{obs,i} - AET_{sim,i})}{\sum_{i=1}^n AET_{obs,i}} * 100 \tag{4}$$

$$NSE = \frac{\sum_{i=1}^n (AET_{obs,i} - AET_{sim,i})^2}{\sum_{i=1}^n (AET_{obs,i} - \overline{AET_{obs,i}})^2} \tag{5}$$

where $AET_{obs,i}$ and $AET_{sim,i}$ are the observed and simulated AET values, respectively, and $\overline{AET_{obs}}$ and $\overline{AET_{sim}}$ are the average observed and simulated AET. R2 ranges from 0 to 1, PBIAS between -100% to $+100\%$ and NSE from $-\infty$ to 1. The optimal values for each one are 1, 0 and 1, respectively.

Aquifer type (A)

Parameter A assesses the lithology of the aquifer, considering that larger grain sizes increase permeability and a higher vulnerability level. Initially, IGME’s geological map of Spain and Portugal at scale 1:1,000,000 was used as the first step in lithology field reconnaissance of worse-defined areas. No changes in A were considered during the studied period because the variations in the geological formation are only visible on a much longer time scale.

Soil type (S)

The amount of recharge, potential dispersion, and filtration process of contamination are influenced by soil. Fine soil or organic content in soil materials can reduce permeability and slow contaminant movement (Yin et al. 2013). The upper altered fraction of soil where biologic activity performs is considered to assess this parameter. As in the previous factor, IGME’s geological map of Spain and Portugal at scale 1:1,000,000 was used, considering no variations in the studied period.

Topography (T)

This parameter considers the slope of the terrain: the higher the slope is, the lower the infiltration results and, consequently, the vulnerability of aquifer contamination. Slope maps during the studied period were obtained using the sources previously referred to in the SWAT model. Notwithstanding, T is the parameter with the lowest effect on DVI.

Impact of vadose zone (I)

The non-saturated zone influences the slowing down of the recharge of the aquifer. This parameter distinguishes between unconfined, semiconfined, and confined aquifers by considering the type of soil in the non-saturated zone. As such, the impact of the vadose zone is determined by its permeability and attenuation characteristics. The parameter I was obtained from IGME’s lithostratigraphic map at scale 1:200,000.

Hydraulic conductivity (C)

Hydraulic conductivity was obtained from a 1×1 spatial resolution map of Spain’s hydraulic conductivity implemented by the University of Leon (Ferrer-Julia et al. 2021).

DVI calculation

The DVI is obtained using Eq. 6 (Aller and Thornhill 1987). In addition to the 1–10 rate for each parameter, its influence within the index is weighted from 1 to 5. Both indices (rate and weight) are multiplied, and the seven values are summed to obtain DVI.

$$\text{DRASTIC Index (DVI)} = (\text{DrDw}) + (\text{RrRw}) + (\text{ArAw}) + (\text{SrSw}) + (\text{TrTw}) + (\text{IrIw}) + (\text{CrCw}) \tag{6}$$

where r and w refer to the rate and weight, respectively. Table 3 show the values of both indices for each parameter.

Table 3 DRASTIC parameters ranges, ratings and weights

Parameter	Range	Rating	Weight
Depth to water (D)	0–1.5	10	5
	1.5–4.5	9	
	4.5–9.1	7	
	9.1–15.1	5	
	15.1–22.9	3	
	22.9–30.5	2	
	> 30.5	1	
	Recharge (R)	0–50.8	
50.8–101.6		3	
101.6–177.8		6	
177.8–254		8	
> 254		9	
Aquifer type (A)	Metamorphic/ Igneous	2–5	3
	Massive sandstone	4–9	
	Sand and gravel	4–9	
Soil type (S)	Sand	9	2
	Sandy loam	6	
	Clay loam	3	
Topography (T)	0–2	10	1
	2–6	9	
	6–12	5	
	12–18	3	
	> 18	1	
Impact vadose zone (I)	Igneous (low permeability)	4	5
	Igneous (medium permeability)	6	
	Sand and gravel with silt and clay	8	
Hydraulic conductivity (C)	0.04–4.1	1	3
	4.1–12.2	2	
	12.2–28.5	4	
	28.5–40.7	6	
	40.7–81.5	8	
	> 81.5	10	

Table 4 Classification of degree of vulnerability

DVI	Degree of vulnerability
66–87	Very low
87–101	Low
101–111	Moderate
111–125	High
125–145	Very high

Finally, spatial DVI is divided into five categories using geometrical interval classification (Table 4) according to the degree of vulnerability obtained (Kazakis and Voudouris 2015). Using GIS techniques, the DVI is calculated for each of the analysed periods (PRE, POST, and PRESENT), and the spatial and temporal evolution of the vulnerability of the aquifer is assessed.

Results and discussion

Depth to water (D)

Figure 3 shows the evolution of the piezometric level during the study period. Regardless of the year, the deepest levels are found in the northern area of the aquifer, reaching over 30 m, so the influence on vulnerability here is thus lower than in the rest of the watershed. It is also common in the three periods that the western-eastern gradient concurring with the drainage net reaches depths lower than 1.5 m in the proximity to the discharge into the Mar Menor. The depth of the phreatic level has been clearly decreasing, particularly on downstream flood plains. Mean depth has gone from around 25 m in the PRE period to 20 and 15 m in the POST and PRESENT periods, respectively. Before the Tajo-Segura water transfer came into operation, crop irrigation derived mainly from groundwater wells, helped by the technological advances that allowed water withdrawals at greater depths and in large amounts (Castejón-Porcel et al.

Fig. 3 Rated/Weighted and Values for DRASTIC factors: D Depth to water table, R Recharge, A Aquifer, S Soil, T Topography, I Impact of Vadose zone, and C Conductivity

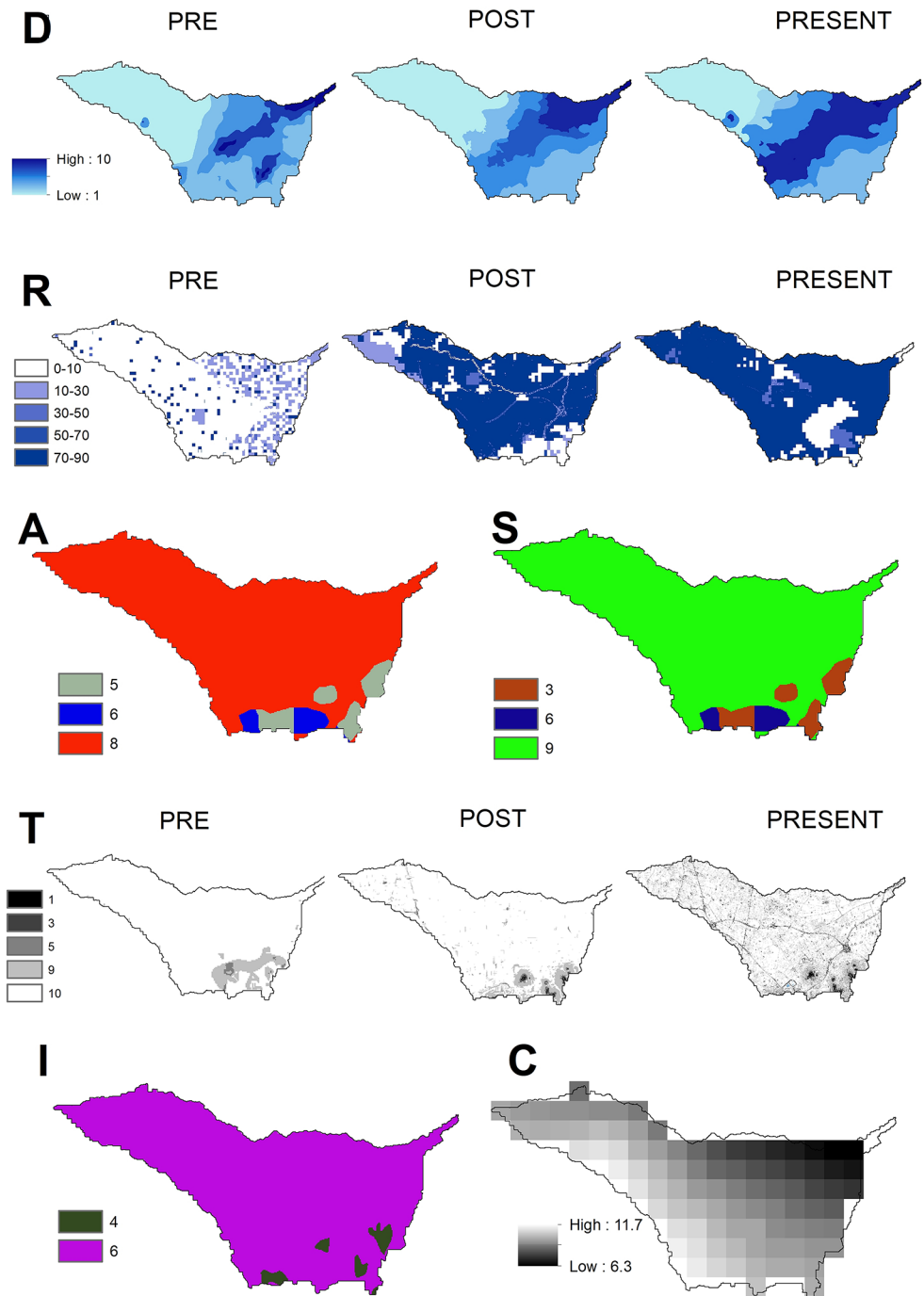


Table 5 SWAT parameters for calibration of AET

Parameter	Default value	Calibrated value
ESCO.hru	0.95	0.80
CN2.mgt	-	+ 5.8%
EPCO.hru	1	0.07
SOL_AWC.sol	-	-9.72%
SOL_Z.sol	-	-15.00%
RCHRG_DP.gw	0.02	0.40

2018). The implementation of water transfer in 1979 caused the water table to rise due to the reduction of extractions and the irrigation returns (Jiménez-Martínez et al. 2016).

Net recharge (R)

As stated above, the SWAT model was used to assess the net recharge in aquifer in the three periods studied. Table 5 shows the fitted values for the most sensitive parameters in the hydrological model when AET satellite-derived data

were compared to SWAT-simulated values. SWAT model monthly performance was satisfactory in both the calibration (2003–2012) and validation (2013–2019) periods according to Moriasi et al. (2007) and Kouchi et al. (2017), as shown in Table 6.

Although average yearly rainfall was similar in the three studied periods (294 mm/year in PRE period, 277 mm/year in POST period and 253 mm/year in the PRESENT period), the average net recharge in the PRE period (4.08 mm/year) was far lower from the more recent periods (26.58 and 21.89 mm/year in POST and PRESENT, respectively) increasing from 1.39% in the 1960s to 9.12% after the water transfer came into operation. According to Abunada (2021), SWAT provides a good representation of the temporal and spatial variability of recharge through the HRU concept, which combines cells with similar hydrological parameters such as slope, land use, soil type and climatic conditions. In the three periods studied (PRE, POST, and PRESENT), land use and climatic conditions vary over time, while slope and soil types are considered static due to their longer-term variation dynamics (López-Ballesteros et al. 2023). Therefore, although the annual climatic conditions in the study area are stable, anthropogenic changes in land use over the years have modified the recharge rate. As a result of the increase in agricultural activity, aquifer recharge increased significantly in irrigated areas (Baudron et al. 2014).

Aquifer type (A)

The Miranda basin presents a high degree of homogeneity with regard to the lithology of the aquifer. More than 80% of the surface is constituted by sand and gravel, typical of floodplains at these latitudes, which explains, the high values of vulnerability associated with this parameter (Fig. 3). Due to the presence of volcanic materials, limestone, and sandstone, the south and southeast areas of the basin are considered of lesser vulnerability.

Soil type (S)

As Fig. 3, demonstrates similar situation to the preceding one holds true regarding soil. Only the clay loam located in the southeast represents something of a barrier against aquifer contamination. Notwithstanding, being at the higher

altitudes of the basin, outside of the floodplain, this area is not suited to cultivation and its anthropisation is less severe.

Topography (T)

The studied basin has a relatively flat landscape, with slopes ranging from 0 to 2%, which makes the aquifer very vulnerable after heavy rains. In the southeast of the Miranda basin, high irregularities are observed due to the presence of some small hills with elevations of around 150 MAMSL; this area is thus less vulnerable in terms of parameter T. The anthropic transformation of land use (roads, urban centres, etc.) has led to an increase in the slope in some parts of the basin, particularly in the present period, as Fig. 3 demonstrates.

Impact of vadose zone (I)

As with the A and S parameters, the low permeability of volcanic rocks in southern and higher-altitude areas represents less than 10% of the Miranda basin, as shown in Fig. 3. The rest of the area is covered with medium permeability soils, such as silty and clay sands that provide intermediate values in the range of the I parameter.

Hydraulic conductivity (C)

According to Ferrer-Julia (2021), hydraulic conductivity in the Miranda basin has, in general, low values, ranging from 6 m/day in the west area to 12 m/day in the east. The spatial distribution is quite homogenous, particularly as we come to the outlet of the wadi into the Mar Menor lagoon. As such, the entire study area has a unique C-parameter value of 2, which is associated with low contamination risk regarding permeability.

Nitrate analysis to validate DRASTIC vulnerability maps

The validation of vulnerability maps is necessary to verify the accuracy and reliability of the vulnerability assessment. This helps ensure that the vulnerability maps are based on sound scientific principles and that they provide a realistic representation of the actual vulnerability of the aquifer. The validation process involves comparing the vulnerability map with the actual occurrence of some common pollutant in groundwater, such as nitrates (Ourarhi et al. 2024a) and pesticides (Zghibi et al. 2016). This comparison helps determine the accuracy of the vulnerability assessment and identify any areas where the vulnerability map may need to be revised or updated. As Fig. 4 demonstrates, the most recent available data have been used to check the correlation between the observed nitrate values and the vulnerability

Table 6 SWAT model performance statistics (satisfactory thresholds according Moriasi et al. 2007 and Kouchi et al. 2017)

Statistic	Calibration	Validation	Satisfactory thresholds
R2	0.75	0.69	> 0.60
KGE	0.63	0.63	≥ 0.50
NSE	0.71	0.66	> 0.50
PBIAS	2.31	2.34	≤ ±20%

Fig. 4 Comparison between DRASTIC vulnerability mapping and observed nitrate concentrations in the study area

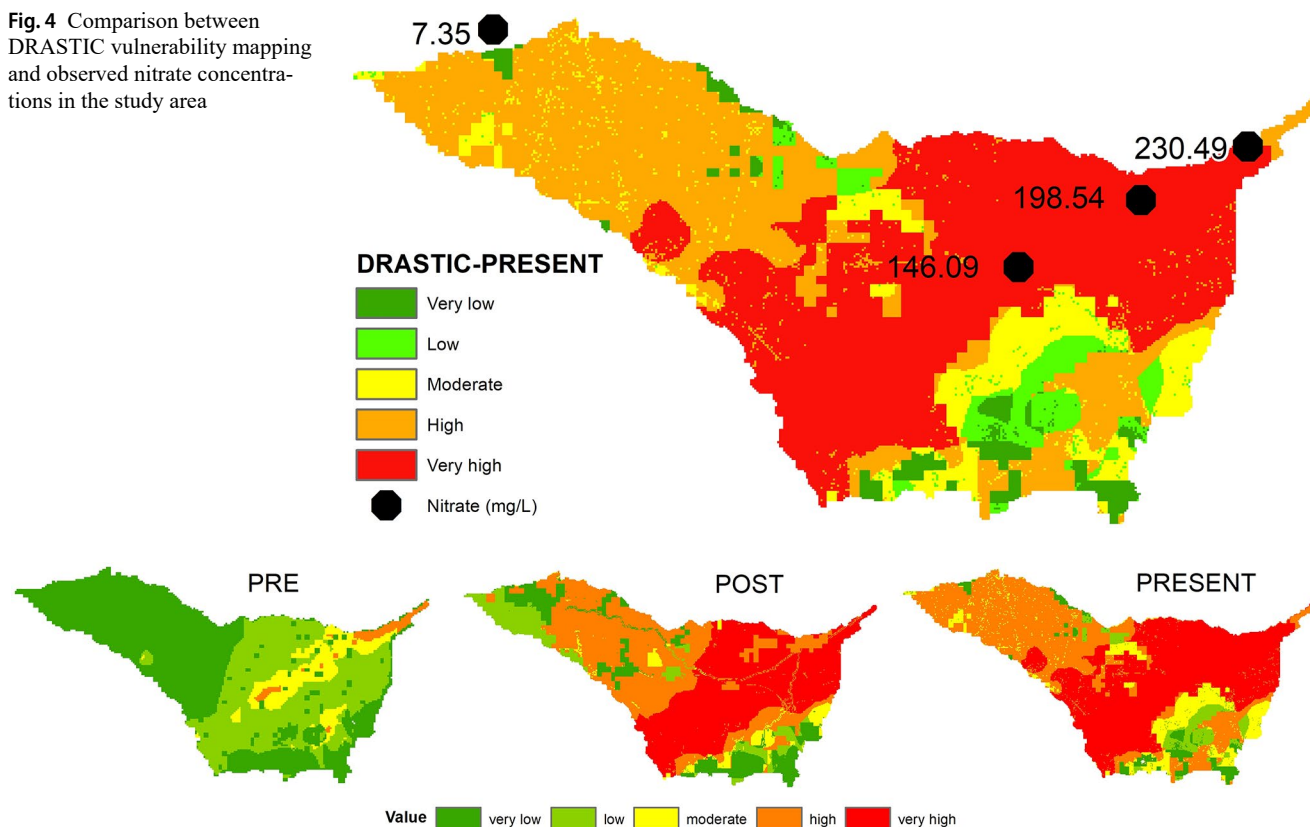


Fig. 5 Spatio-temporal evolution of DVI

map values; this reveals a strong relationship between them ($R^2 = 0.86$). This analysis confirms that the estimated vulnerability map aligns with the real distribution of nitrates in the aquifer. As expected, the highest concentrations of nitrates in groundwater (over 100 mg/L) are found in the areas near the mouth of the basin, where there is a concentration of cultivated areas for horticultural crops. Conversely, the lowest values observed (7.35 mg/L) are located around the town of Albuñón (headwaters of the Miranda basin), where agricultural activity is non-existent.

In recent years, and due to the serious environmental deterioration of the Mar Menor, great efforts have been made to monitor the lagoon. However, the situation in the CC watershed and aquifer differs completely. Here, there are few gauging stations to measure the flows caused by storms (Cecilia et al. 2023), and the network for monitoring piezometric levels and the amount of nitrates in the aquifer present serious problems of representativeness; most of the wells are privately owned, which hinders access to them and limits information on recent pumping activities and on the operational status of the pump (García-Aróstegui et al. 2024). This has led to little information being available for the validation of the vulnerability maps, which is a limitation of this study that can be improved upon in future work when more data are available.

Evolution of vulnerability

After calculating the six parameters of the DRASTIC method for each of the three periods under study, the weights in Table 4 were applied and the evolution of DVI was assessed, as Fig. 5 demonstrates. Amongst all the parameters, A, S, I, and C had no influence on the evolution, thus were considered invariable, as justified above. Furthermore, the differences in those parameters in the watershed appear in the southern boundaries, which coincides with the highest altitudes where agricultural activities are scarce. As such, the main factors were D, R and T. The latter is related to the development of road infrastructure and buildings linked to farming areas, but their extension is limited to small areas of land, as in Fig. 3 demonstrates. Finally, the most influential parameters were D and R as such, besides having the highest weights in DVI, their values have also significantly changed during the periods referred to. On the one hand, the piezometric level has risen, on average, between 5 and 10 m from the PRE to the POST period, which highlights the trends of DVI evolution shown in Fig. 5. On the other hand, the net recharge, which began nearly started from scratch in the PRE period due to the large withdrawals of water, reached around 24 mm/year after the water transfer came

into operation, which enabled the dragging and filtration of plant protection products (Senent-Aparicio et al. 2015).

The Tajo-Segura water transfer led to an increase of groundwater recharge and an important recovery of water tables. However, this fact, which might be considered, a priori, as positive in the environmental aquifer status, has turned out to be a growing vulnerability with regards to contamination. This, together with the massive expansion of irrigated crops in the area since the Tagus-Segura transfer came into operation (Jiménez-Martínez et al. 2016; Domingo-Pinillos et al. 2018), has already had a major impact on Mar Menor eutrophication (Jimeno-Sáez et al. 2020; Álvarez-Rogel et al. 2020; Sandonini et al. 2021).

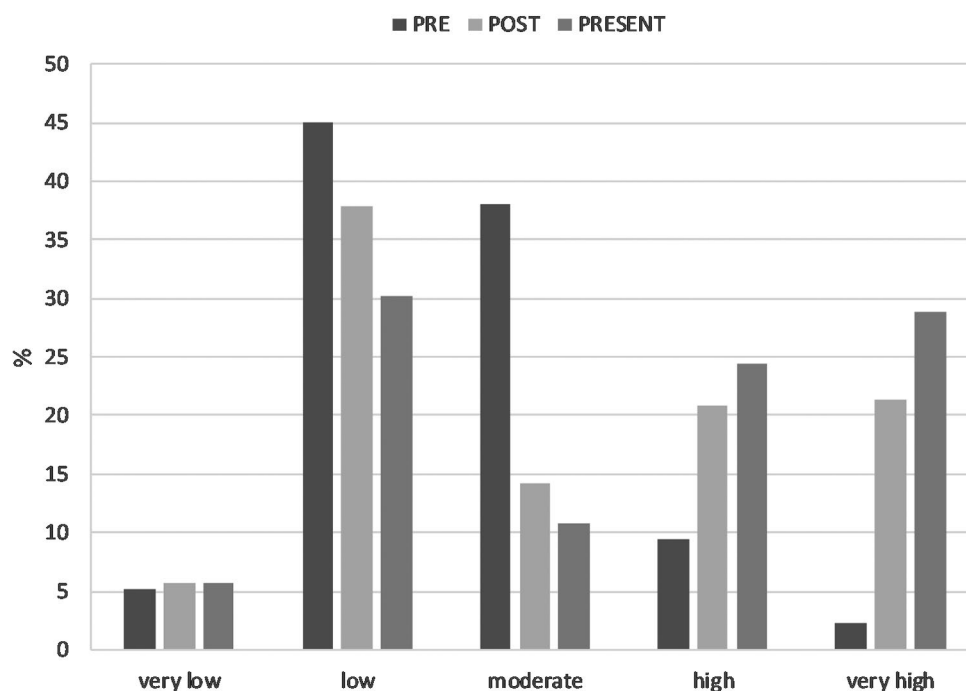
The evolution of vulnerability in the aquifer has been strongly associated with the development of farming in the area. As crop irrigation has spread along the alluvial plains of the watershed in the southeastern-southwestern direction, high vulnerability values have been expanding, particularly in the lowest altitudes and slopes, where conditions for cultivation are clearly optimal. Furthermore, the location of crops in floodplains together with a soil structure, favourable to filtration to lower layers, has contributed to a rapid and high degree of aquifer vulnerability, starting from the drainage net of the watershed. Predictably, the higher the altitudes are, the lower the variations and vulnerability are. In fact, the north area of the basin remained in low vulnerability in the three periods, and the very low values in the mountainous boundaries in the south did not change in any scenario.

Figure 6 shows the percentages of each degree of vulnerability in the periods studied. As stated above, the

vulnerability of the Miranda basin aquifer has clearly evolved negatively since the Tagus-Segura water transfer came into operation. Initially, more than 50% of the watershed had low values and only 12% of the area could be considered highly vulnerable. The water transfer has a clearly negative effect on aquifer vulnerability since its inception, as reflected in the 1990 period. Whereas the difference in lowest classes in 1990 (very low and low) did not reach 7% compared with previous period, there was a drastic decrease in moderate class (around 24%), which increased significantly high (11%) and, in particular, very high vulnerability (20%) in aquifer. The last period reflects the continuation of the past trend, reaching over 53% of the total watershed for the most vulnerable classes, at the expense of reducing the moderate and low vulnerability classes by more than 11%. The very low vulnerability percentage has remained practically unchanged since the 1960s (around 5%) because it represents the mountainous area where crop irrigation is nearly non-existent.

The quality status of groundwater resources in the Miranda basin is relevant, for not only for a sustainable agricultural production but also the environmental status of the aquifer and the coastal lagoon of the Mar Menor, which drains into. Changes in agricultural practices in the Miranda drainage basin together with the introduction of intensive irrigation crops, have substantially modified its sensitivity to contamination, as evidenced by the processes of eutrophication and degradation of water quality in the Mar Menor at present (Erena et al. 2019; Jimeno-Sáez et al. 2020; Guaita-García et al. 2022). Restrictions related to soil fertilisation, permanent pastures or afforestation should

Fig. 6 Evolution of aquifer vulnerability by class/surface area (%)



be imposed in areas with high vulnerability indices to slow down and reverse this situation, as recommended in similar studies (Ourarhi et al. 2022). Furthermore, moderately vulnerable areas require ongoing monitoring to manage the consequences resulting from intensive agriculture.

Conclusions

The anthropogenic modification of land uses and their impact analysis on aquifers are essential tools for understanding degradation trends in both water quality and quantity, as well as the threat to the biodiversity of associated ecosystems. This study presents a novel application of the DRASTIC method to evaluate the temporal evolution of aquifer vulnerability at three key historical moments, which emphasises the significant influence of human activities on the current degradation of the aquifer. This temporal evaluation allows for a precise spatial definition of its improvement or deterioration over the analysed periods and provides a dynamic view of the cumulative impacts of human interventions.

Evaluating the DVI in historical contexts presents significant challenges, particularly due to the lack of detailed data and changes in land use over time. However, the evolution of the Miranda basin, which has undergone drastic changes in agricultural production structures over the last 70 years, illustrates the profound impact of human activities on the aquifer. Changes in crop types, land use restructuring, and water resource management, partly driven by the Tajo-Segura water transfer, have significantly transformed the vulnerability of the aquifer. The extent of high vulnerability areas drastically increased, from 11% in the PRE period to 53% in the PRESENT period, while low and moderate vulnerability areas decreased by 15% and 28%, respectively. These results underscore the importance of temporal evaluation and reveal how anthropogenic actions have exacerbated vulnerability over time. While geological and geomorphological parameters have remained virtually unchanged, changes in aquifer recharge and piezometric levels have been key factors in the current greater vulnerability of the aquifer.

The estimation of aquifer recharge through the widely validated SWAT hydrological model has enabled the generation of reliable maps depicting this critical parameter and facilitated a more accurate assessment of vulnerability evolution. SWAT has proven to be a robust tool for simulating complex hydrological processes by integrating extensive data and advanced algorithms that allow for the evaluation of diverse land use scenarios. By operating at the scale of (HRUs), SWAT captures the spatial variability

of hydrological processes, which is particularly useful in regions with complex dynamics, such as the Miranda basin.

The implications of this research extend beyond local applications and significantly enhance the scientific understanding of aquifer vulnerability within global water management challenges. As water scarcity and pollution increasingly threaten ecosystems worldwide, this study emphasises the urgent need for sustainable land use and resource management practices. The developed methodology is adaptable to various geographical contexts, which highlights its global relevance. This research ultimately equips policymakers with essential insights and tools for effective water management that emphasise the need for continuous monitoring and land use restrictions to mitigate vulnerability.

Author contributions Francisco J. Segura-Méndez: Conceptualization, Writing – original draft. Julio Pérez-Sánchez: Writing – original draft. Adrián López-Ballesteros: Data curation. Javier Senent-Aparicio: Writing – original draft, Funding acquisition, Supervision.

Funding This work was supported by the European Union's Horizon 2020 research and innovation programme within the framework of the project SMARTLAGOON, grant agreement number 101017861.

Data availability No datasets were generated or analysed during the current study.

Declarations

Ethics approval and consent to participate Not applicable.

Consent for publication Not applicable.

Competing interests The authors declare no competing interests.

References

- Abdelshafy M, Saber M, Abdelhaleem A et al (2019) Hydrogeochemical processes and evaluation of groundwater aquifer at Sohag City. *Egypt Sci Afr* 6:e00196. <https://doi.org/10.1016/j.sciaf.2019.e00196>
- Abunada Z, Kishawi Y, Alslaibi TM et al (2021) The application of SWAT-GIS tool to improve the recharge factor in the DRASTIC framework: case study. *J Hydrol* 592:125613. <https://doi.org/10.1016/j.jhydrol.2020.125613>
- Ahada CPS, Suthar S (2018) A GIS based DRASTIC model for assessing aquifer vulnerability in Southern Punjab, India. *Model Earth Syst Environ* 4:635–645. <https://doi.org/10.1007/s40808-018-0449-6>
- Ahmed SI, Cheng C-L, Gonzalez J et al (2022) Groundwater vulnerability assessment of shallow aquifer in the South Texas sand sheet using a GIS-based DRASTIC model. *Model Earth Syst Environ* 8:4075–4091. <https://doi.org/10.1007/s40808-021-01292-4>
- Albuquerque MTD, Sanz G, Oliveira SF et al (2013) Spatio-temporal Groundwater Vulnerability Assessment - A coupled remote sensing and GIS Approach for historical Land Cover Reconstruction.

- Water Resour Manage 27:4509–4526. <https://doi.org/10.1007/s1269-013-0422-0>
- Aller L, Thornhill J (1987) DRASTIC: a standardized system for evaluating ground water pollution potential using hydrogeologic settings. Robert S. Kerr Environmental Research Laboratory, Office of Research and …
- Álvarez-Rogel J, Barberá GG, Maxwell B et al (2020) The case of Mar Menor eutrophication: state of the art and description of tested nature-based solutions. *Ecol Eng* 158:106086. <https://doi.org/10.1016/j.ecoleng.2020.106086>
- Amarni N, Fernane L, Naili M et al (2020) Mapping of the vulnerability to marine intrusion in coastal Cherchell aquifer, Central Algeria using the GALDIT method. *Groundw Sustainable Dev* 11:100481. <https://doi.org/10.1016/j.gsd.2020.100481>
- Ameur M, Aouiti S, Hamzaoui-Azaza F et al (2021) Vulnerability assessment, transport modeling and simulation of nitrate in groundwater using SI method and modflow-MT3DMS software: case of Sminja aquifer, Tunisia. *Environ Earth Sci* 80:220. <https://doi.org/10.1007/s12665-021-09491-z>
- Arnold JG, Srinivasan R, Muttiah RS, Williams JR (1998) Large Area Hydrologic modeling and Assessment Part I: Model Development. *J Am Water Resour Assoc* 34:73–89. <https://doi.org/10.1111/j.1752-1688.1998.tb05961.x>
- Asadi P, Ataie-Ashtiani B, Beheshti A (2016) Vulnerability assessment of urban groundwater resources to nitrate: the case study of Mashhad, Iran. *Environ Earth Sci* 76:41. <https://doi.org/10.1007/s12665-016-6357-z>
- Banerjee A, Creedon L, Jones N et al (2023) Dynamic Groundwater Contamination Vulnerability Assessment techniques: a systematic review. *Hydrology* 10:182. <https://doi.org/10.3390/hydrology10090182>
- Baudron P, Barbecot F, Aróstegui JLG et al (2014) Impacts of human activities on recharge in a multilayered semiarid aquifer (Campo De Cartagena, SE Spain). *Hydrol Process* 28:2223–2236. <https://doi.org/10.1002/hyp.9771>
- Bera A, Mukhopadhyay BP, Chowdhury P et al (2021) Groundwater vulnerability assessment using GIS-based DRASTIC model in Nangasai River Basin, India with special emphasis on agricultural contamination. *Ecotoxicol Environ Saf* 214:112085. <https://doi.org/10.1016/j.ecoenv.2021.112085>
- Bhattarai N, Pollack A, Lobell DB et al (2021) The impact of groundwater depletion on agricultural production in India. *Environ Res Lett* 16:085003. <https://doi.org/10.1088/1748-9326/ac10de>
- Bowman DMJS, Balch J, Artaxo P et al (2011) The human dimension of fire regimes on Earth. *J Biogeogr* 38:2223–2236. <https://doi.org/10.1111/j.1365-2699.2011.02595.x>
- Busico G, Kazakis N, Cuoco E et al (2020) A novel hybrid method of specific vulnerability to anthropogenic pollution using multivariate statistical and regression analyses. *Water Res* 171:115386. <https://doi.org/10.1016/j.watres.2019.115386>
- Castejón-Portel G, Espín-Sánchez D, Ruiz-Álvarez V et al (2018) Runoff Water as a resource in the Campo De Cartagena (Region of Murcia): current possibilities for Use and benefits. *Water* 10:456. <https://doi.org/10.3390/w10040456>
- Cecilia J, Hernández D, Arratia B et al (2023) In situ and crowd-sensing techniques for monitoring flows in Ephemeral streams. *IEEE Network* 37:310–317. <https://doi.org/10.1109/MNET.005.2200545>
- CHS (2022) The American Flight of 1956 (USAF56) in the Segura Basin. <https://www.chsegura.es/en/cuenca/cartografia/servicios-web-de-mapas/vuelo-americano-de-1956/index.html> (accessed 4 January 2022)
- Chuai X, Chen X, Yang L et al (2012) Effects of climatic changes and anthropogenic activities on lake eutrophication in different ecoregions. *Int J Environ Sci Technol* 9:503–514. <https://doi.org/10.1007/s13762-012-0066-2>
- Claus Henn B, Ogneva-Himmelberger Y, Denehy A et al (2018) Integrated Assessment of shallow-aquifer vulnerability to multiple contaminants and drinking-water exposure pathways in Holliston, Massachusetts. *Water* 10:23. <https://doi.org/10.3390/w10010023>
- Congedo L (2021) Semi-automatic classification Plugin: a Python tool for the download and processing of remote sensing images in QGIS. *J Open Source Softw* 6:3172. <https://doi.org/10.21105/joss.03172>
- Cook J, Oreskes N, Doran PT et al (2016) Consensus on consensus: a synthesis of consensus estimates on human-caused global warming. *Environ Res Lett* 11:048002. <https://doi.org/10.1088/1748-9326/11/4/048002>
- Cudennec C, Leduc C, Koutsoyiannis D (2007) Dryland hydrology in Mediterranean regions—a review. *Hydrol Sci Journal/Journal Des Sci Hydrol*. <https://doi.org/10.1623/hysj.52.6.1077>
- Custodio Gimena E, Andreu Rodes JM, Aragón Rueda R et al (2016) Groundwater intensive use and mining in south-eastern peninsular Spain: hydrogeologic-economic and social aspects. <https://doi.org/10.1016/j.scitotenv.2016.02.107>
- Dhaouadi L, Besser H, karbout N et al (2021) Assessment of natural resources in Tunisian oases: degradation of irrigation water quality and continued overexploitation of groundwater. *Euro-Mediterr J Environ Integr* 6:36. <https://doi.org/10.1007/s41207-020-00234-3>
- Domingo-Pinillos JC, Senent-Aparicio J, García-Aróstegui JL, Baudron P (2018) Long Term Hydrodynamic effects in a Semi-arid Mediterranean Multilayer Aquifer: Campo De Cartagena in South-Eastern Spain. *Water* 10:1320. <https://doi.org/10.3390/w10101320>
- du Plessis A (2019) Current and future water scarcity and stress. In: du Plessis A (ed) *Water as an inescapable risk: current global water availability, quality and risks with a specific focus on South Africa*. Springer International Publishing, Cham, pp 13–25
- Ekanem AM (2022) AVI- and GOD-based vulnerability assessment of aquifer units: a case study of parts of Akwa Ibom State, Southern Niger Delta, Nigeria. *Sustain Water Resour Manag* 8:29. <https://doi.org/10.1007/s40899-022-00628-x>
- Ellis EC (2015) Ecology in an anthropogenic biosphere. *Ecol Monogr* 85:287–331. <https://doi.org/10.1890/14-2274.1>
- Erena M, Domínguez JA, Aguado-Giménez F et al (2019) Monitoring Coastal Lagoon Water Quality through Remote sensing: the Mar Menor as a case study. *Water* 11:1468. <https://doi.org/10.3390/w11071468>
- Eslamian S, Harooni Y, Sabzevari Y (2023) Simulation of nitrate pollution and vulnerability of groundwater resources using MODFLOW and DRASTIC models. *Sci Rep* 13:8211. <https://doi.org/10.1038/s41598-023-35496-8>
- Fannakh A, Farsang A (2022) DRASTIC, GOD, and SI approaches for assessing groundwater vulnerability to pollution: a review. *Environ Sci Eur* 34:77. <https://doi.org/10.1186/s12302-022-00646-8>
- Ferrer-Julia M, García-Meléndez E, Alcalde-Aparicio S (2021) Mapping saturated hydraulic conductivity from open-access soil databases. *CATENA* 197:104973. <https://doi.org/10.1016/j.catena.2020.104973>
- García-Aróstegui J-L, Baudron P, Robles-Arenas VM (2024) Sampling methods may drive short-term groundwater nitrate variability in an irrigated watershed connected to a coastal lagoon (Campo De Cartagena-Mar Menor, SE Spain). *Sci Total Environ* 912:169188. <https://doi.org/10.1016/j.scitotenv.2023.169188>
- Geng C, Lu D, Qian J et al (2023) A review on process-based Groundwater Vulnerability Assessment methods. *Processes* 11:1610. <https://doi.org/10.3390/pr11061610>
- Ghaleni M, Ebrahimi K (2015) Effects of human activities and climate variability on water resources in the Saveh plain, Iran. *Environ Monit Assess* 187:35. <https://doi.org/10.1007/s10661-014-4243-2>

- Guita-García N, Martínez-Fernández J, Barrera-Causil CJ, Fitz HC (2022) Stakeholder analysis and prioritization of management measures for a sustainable development in the social-ecological system of the Mar Menor (SE, Spain). *Environ Dev* 42:100701. <https://doi.org/10.1016/j.envdev.2022.100701>
- Gupta HV, Kling H, Yilmaz KK, Martinez GF (2009) Decomposition of the mean squared error and NSE performance criteria: implications for improving hydrological modelling. *J Hydrol* 377:80–91. <https://doi.org/10.1016/j.jhydrol.2009.08.003>
- Hagner O, Reese H (2007) A method for calibrated maximum likelihood classification of forest types. *Remote Sens Environ* 110:438–444. <https://doi.org/10.1016/j.rse.2006.08.017>
- Hajji S, Allouche N, Bouri S et al (2022) Assessment of seawater intrusion in Coastal aquifers using Multivariate statistical analyses and hydrochemical facies evolution-based model. *Int J Environ Res Public Health* 19:155. <https://doi.org/10.3390/ijerph19010155>
- Hautier Y, Tilman D, Isbell F et al (2015) Anthropogenic environmental changes affect ecosystem stability via biodiversity. *Science* 348:336–340. <https://doi.org/10.1126/science.aaa1788>
- Ibarra Marinas D, Belmonte Serrato F, Rubio Iborra J (2017) El Impacto territorial del uso agrícola y turístico del litoral: evolución De Los cambios de uso del suelo en las cuencas litorales del sur de la Región de Murcia (1956–2013). *Boletín de la Asociación de Geógrafos Españoles*. <https://doi.org/10.21138/bage.2419>
- Idowu TE, Jepakosgei C, Nyadawa M et al (2022) Integrated seawater intrusion and groundwater quality assessment of a coastal aquifer: GALDIT, geospatial and analytical approaches. *Environ Sci Pollut Res* 29:36699–36720. <https://doi.org/10.1007/s11356-021-18084-z>
- Iglesias A, Garrote L, Flores F, Moneo M (2007) Challenges to manage the risk of Water Scarcity and Climate Change in the Mediterranean. *Water Resour Manage* 21:775–788. <https://doi.org/10.1007/s11269-006-9111-6>
- Ikenna IS, Chinedu EE, Chibuie IE (2021) A SINTACS GIS-based method for assessing groundwater vulnerability in sedimentary aquifers, South-Eastern, Nigeria. *Arab J Geosci* 14:733. <https://doi.org/10.1007/s12517-021-07092-5>
- Issaka S, Ashraf MA (2017) Impact of soil erosion and degradation on water quality: a review. *Geol Ecol Landscapes* 1:1–11. <https://doi.org/10.1080/24749508.2017.1301053>
- Jafarzadeh F, Asghari Moghaddam A, Razzagh S et al (2024) A meta-ensemble machine learning strategy to assess groundwater holistic vulnerability in coastal aquifers. *Groundw Sustainable Dev* 26:101296. <https://doi.org/10.1016/j.gsd.2024.101296>
- Jahromi MN, Gomesh Z, Busico G et al (2021) Developing a SINTACS-based method to map groundwater multi-pollutant vulnerability using evolutionary algorithms. *Environ Sci Pollut Res* 28:7854–7869. <https://doi.org/10.1007/s11356-020-11089-0>
- Jakeman AJ, Barreteau O, Hunt RJ et al (2016) Integrated Groundwater Management: an overview of concepts and challenges. In: Jakeman AJ, Barreteau O, Hunt RJ et al (eds) *Integrated Groundwater Management: concepts, approaches and challenges*. Springer International Publishing, Cham, pp 3–20
- Jang C-S (2022) Aquifer vulnerability assessment for fecal coliform bacteria using multi-threshold logistic regression. *Environ Monit Assess* 194:800. <https://doi.org/10.1007/s10661-022-10481-2>
- Jansen LJM, Gregorio AD (2002) Parametric land cover and land-use classifications as tools for environmental change detection. *Agric Ecosyst Environ* 91:89–100. [https://doi.org/10.1016/S0167-8809\(01\)00243-2](https://doi.org/10.1016/S0167-8809(01)00243-2)
- Jiménez-Martínez J, García-Aróstegui JL, Hunink JE et al (2016) The role of groundwater in highly human-modified hydrosystems: a review of impacts and mitigation options in the Campo De Cartagena-Mar Menor coastal plain (SE Spain). *Environ Rev* 24:377–392. <https://doi.org/10.1139/er-2015-0089>
- Jimeno-Sáez P, Senent-Aparicio J, Cecilia JM, Pérez-Sánchez J (2020) Using machine-learning algorithms for Eutrophication modeling: Case Study of Mar Menor lagoon (Spain). *IJERPH* 17:1189. <https://doi.org/10.3390/ijerph17041189>
- Kazakis N, Voudouris KS (2015) Groundwater vulnerability and pollution risk assessment of porous aquifers to nitrate: modifying the DRASTIC method using quantitative parameters. *J Hydrol* 525:13–25. <https://doi.org/10.1016/j.jhydrol.2015.03.035>
- Kouchi DH, Esmaili K, Faridhosseini A et al (2017) Sensitivity of Calibrated Parameters and Water Resource estimates on different objective functions and optimization algorithms. *Water* 9:384. <https://doi.org/10.3390/w9060384>
- Kwon E, Park J, Park W-B et al (2022) Nitrate vulnerability of groundwater in Jeju Volcanic Island, Korea. *Sci Total Environ* 807:151399. <https://doi.org/10.1016/j.scitotenv.2021.151399>
- Lai Y, Wang F, Zhang Y et al (2019) Implementing chemical mass balance model and vulnerability theories to realize the comprehensive evaluation in an abandoned battery plant. *Sci Total Environ* 686:788–796. <https://doi.org/10.1016/j.scitotenv.2019.05.025>
- Lapworth DJ, Boving TB, Kreamer DK et al (2022) Groundwater quality: global threats, opportunities and realising the potential of groundwater. *Sci Total Environ* 811:152471. <https://doi.org/10.1016/j.scitotenv.2021.152471>
- Li D, Tian P, Luo Y et al (2021) Importance of stopping groundwater irrigation for balancing agriculture and wetland ecosystem. *Ecol Ind* 127:107747. <https://doi.org/10.1016/j.ecolind.2021.107747>
- López-Ballesteros A, Senent-Aparicio J, Srinivasan R, Pérez-Sánchez J (2019) Assessing the impact of Best Management practices in a highly anthropogenic and ungauged Watershed using the SWAT model: a Case Study in the El Beal Watershed (Southeast Spain). *Agronomy* 9:576. <https://doi.org/10.3390/agronomy9100576>
- López-Ballesteros A, Trolle D, Srinivasan R, Senent-Aparicio J (2023) Assessing the effectiveness of potential best management practices for science-informed decision support at the watershed scale: the case of the Mar Menor coastal lagoon, Spain. *Sci Total Environ* 859:160144. <https://doi.org/10.1016/j.scitotenv.2022.160144>
- Machiwal D, Jha MK, Singh VP, Mohan C (2018) Assessment and mapping of groundwater vulnerability to pollution: current status and challenges. *Earth Sci Rev* 185:901–927. <https://doi.org/10.1016/j.earscirev.2018.08.009>
- Mahrez B, Klebingat S, Houha B, Houria B (2018) GIS-based GALDIT method for vulnerability assessment to seawater intrusion of the quaternary coastal Collo aquifer (NE-Algeria). *Arab J Geosci* 11:1–14. <https://doi.org/10.1007/s12517-018-3400-2>
- Miralles DG, Holmes TRH, De Jeu Ra. M, et al (2011) Global land-surface evaporation estimated from satellite-based observations. *Hydrol Earth Syst Sci* 15:453–469. <https://doi.org/10.5194/hess-15-453-2011>
- Moench M (2003) Groundwater and poverty: exploring the connections. *Intensive use of groundwater: Challenges and opportunities* 441–456
- Moriasi DN, Arnold JG, Van Liew MW et al (2007) Model evaluation guidelines for systematic quantification of accuracy in watershed simulations. *Trans ASABE* 50:885–900
- Nazzal Y, Howari FM, Iqbal J et al (2019) Investigating aquifer vulnerability and pollution risk employing modified DRASTIC model and GIS techniques in Liwa area, United Arab Emirates. *Groundw Sustainable Dev* 8:567–578. <https://doi.org/10.1016/j.gsd.2019.02.006>
- Ncibi K, Chaar H, Hadji R et al (2020) A GIS-based statistical model for assessing groundwater susceptibility index in shallow aquifer in Central Tunisia (Sidi Bouzid basin). *Arab J Geosci* 13:98. <https://doi.org/10.1007/s12517-020-5112-7>
- Neitsch SL, Arnold JG, Kiniry JR, Williams JR (2011) *Soil and water assessment tool theoretical documentation version 2009*. Texas Water Resources Institute

- Niemelä J, Kotze J, Ashworth A et al (2000) The search for common anthropogenic impacts on biodiversity: a global network. *J Insect Conserv* 4:3–9
- Noori R, Ghahremanzadeh H, Kløve B et al (2019) Modified-DRASTIC, modified-SINTACS and SI methods for groundwater vulnerability assessment in the southern Tehran aquifer. *J Environ Sci Health Part A* 54:89–100. <https://doi.org/10.1080/10934529.2018.1537728>
- Oke SA (2020) Regional Aquifer Vulnerability and Pollution Sensitivity Analysis of drastic application to Dahomey Basin of Nigeria. *Int J Environ Res Public Health* 17:2609. <https://doi.org/10.3390/ijerph17072609>
- Oni TE, Omosuyi GO, Akinlalu AA (2017) Groundwater vulnerability assessment using hydrogeologic and geoelectric layer susceptibility indexing at Igbara Oke, Southwestern Nigeria. *NRIAG J Astron Geophys* 6:452–458. <https://doi.org/10.1016/j.nrjag.2017.04.009>
- Ouarekh M, Bouselsal B, Belksier MS, Benaabidate L (2021) Water quality assessment and hydrogeochemical characterization of the Complex Terminal aquifer in Souf Valley, Algeria. *Arab J Geosci* 14:1–18. <https://doi.org/10.1007/s12517-021-08498-x>
- Ourarhi S, Barkaoui A-E, Zarhloule Y (2022) Assessment of the Agricultural Intensification Impact on Groundwater Quality: a case study of the Triffa Plain. *Water Air Soil Pollut* 233:342. <https://doi.org/10.1007/s11270-022-05810-7>
- Ourarhi S, Barkaoui A-E, Zarhloule Y et al (2024a) Groundwater vulnerability assessment in the Triffa Plain based on GIS combined with DRASTIC, SINTACS, and GOD models. *Model Earth Syst Environ* 10:619–629. <https://doi.org/10.1007/s40808-023-01801-7>
- Ourarhi S, Barkaoui A-E, Zarhloule Y (2024b) Enhanced methods for evaluating Aquifer susceptibility: incorporating Static and dynamic vulnerability assessments. *Water Resour Manage* 38:2791–2810. <https://doi.org/10.1007/s11269-024-03792-1>
- Ourarhi S, Barkaoui A-E, Zarhloule Y (2024c) Mapping groundwater's susceptibility to pollution in the Triffa Plain (Eastern Morocco) using a modified method based on the DRASTIC, RIVA, and AHP models. *Environ Dev Sustain* 26:15535–15555. <https://doi.org/10.1007/s10668-023-03262-5>
- Ourarhi S, Kadiri M, Barkaoui A-E et al (2024d) Assessment of risk intensity in the triffa plain aquifer: integration of hazard quantification, land use analysis, dynamic vulnerability GCITF, and DRASTIC method. *Groundw Sustainable Dev* 26:101291. <https://doi.org/10.1016/j.gsd.2024.101291>
- Pacheco FAL, Martins LMO, Quininha M et al (2018) Modification to the DRASTIC framework to assess groundwater contaminant risk in rural mountainous catchments. *J Hydrol* 566:175–191. <https://doi.org/10.1016/j.jhydrol.2018.09.013>
- Phok R, Kosgallana Duwage Wasantha N, Sumana Bandara W et al (2021) Using intrinsic vulnerability and anthropogenic impacts to evaluate and compare groundwater risk potential at northwestern and western coastal aquifers of Sri Lanka through coupling DRASTIC and GIS approach. *Appl Water Sci* 11:117. <https://doi.org/10.1007/s13201-021-01452-y>
- Pisciotta A, Cusimano G, Favara R (2015) Groundwater nitrate risk assessment using intrinsic vulnerability methods: a comparative study of environmental impact by intensive farming in the Mediterranean region of Sicily, Italy. *J Geochem Explor* 156:89–100. <https://doi.org/10.1016/j.gexplo.2015.05.002>
- Rezaei F, Safavi HR, Ahmadi A (2013) Groundwater Vulnerability Assessment using fuzzy logic: a Case Study in the Zayandehrood aquifers, Iran. *Environ Manage* 51:267–277. <https://doi.org/10.1007/s00267-012-9960-0>
- Rupérez-Moreno C, Senent-Aparicio J, Martínez-Vicente D et al (2017) Sustainability of irrigated agriculture with overexploited aquifers: the case of Segura basin (SE, Spain). *Agric Water Manage* 182:67–76. <https://doi.org/10.1016/j.agwat.2016.12.008>
- Saaty TL (1988) Some Mathematical topics in the Analytic Hierarchy process. In: Mitra G, Greenberg HJ, Lootsma FA et al (eds) *Mathematical models for decision support*. Springer, Berlin, Heidelberg, pp 89–107
- Sandonnini J, Del Pilar Ruso Y, Cortés Melendreras E et al (2021) The emergent fouling population after severe eutrophication in the Mar Menor coastal lagoon. *Reg Stud Mar Sci* 44:101720. <https://doi.org/10.1016/j.rsma.2021.101720>
- Sarah S, Ahmed S, Violette S, de Marsily G (2021) Groundwater sustainability challenges revealed by quantification of contaminated groundwater volume and aquifer depletion in hard rock aquifer systems. *J Hydrol* 597:126286. <https://doi.org/10.1016/j.jhydrol.2021.126286>
- Schmid T, Koch M, Gumuzzio J (2005) Multisensor approach to determine changes of wetland characteristics in semiarid environments (central Spain). *IEEE Trans Geosci Remote Sens* 43:2516–2525. <https://doi.org/10.1109/TGRS.2005.852082>
- Senarathne S, Jayawardana JMCK, Edirisinghe EANV, Chandrajith R (2021) Geochemical and isotope evidence for groundwater mineralization in a semi-arid river basin, Sri Lanka. *Appl Geochem* 124:104799. <https://doi.org/10.1016/j.apgeochem.2020.104799>
- Senent-Aparicio J, Pérez-Sánchez J, García-Aróstegui JL et al (2015) Evaluating Groundwater Management Sustainability under Limited Data availability in Semiarid zones. *Water* 7:4305–4322. <https://doi.org/10.3390/w7084305>
- Senent-Aparicio J, López-Ballesteros A, Nielsen A, Trolle D (2021) A holistic approach for determining the hydrology of the mar menor coastal lagoon by combining hydrological & hydrodynamic models. *J Hydrol* 603:127150. <https://doi.org/10.1016/j.jhydrol.2021.127150>
- Shah SHIA, Yan J, Ullah I et al (2021) Classification of Aquifer vulnerability by using the DRASTIC Index and Geo-Electrical Techniques. *Water* 13:2144. <https://doi.org/10.3390/w13162144>
- Singh D, Karambelas A, Chhatre A et al (2021) A systems lens to evaluate the compound human health impacts of anthropogenic activities. *One Earth* 4:1233–1247. <https://doi.org/10.1016/j.oneear.2021.08.006>
- Souza V, Mandujano MC, Pisanty I, Eguarte LE (eds) (2022) *Conflicts between Biodiversity Conservation and humans: the case of the Chihuahua Desert and Cuatro Ciénegas*. Springer International Publishing, Cham
- Taghavi N, Niven RK, Paull DJ, Kramer M (2022) Groundwater vulnerability assessment: a review including new statistical and hybrid methods. *Sci Total Environ* 822:153486. <https://doi.org/10.1016/j.scitotenv.2022.153486>
- Testoni R, Levizzari R, De Salve M (2017) Coupling of unsaturated zone and saturated zone in radionuclide transport simulations. *Prog Nucl Energy* 95:84–95. <https://doi.org/10.1016/j.pnucene.2016.11.012>
- Tuomainen U, Candolin U (2011) Behavioural responses to human-induced environmental change. *Biol Rev* 86:640–657. <https://doi.org/10.1111/j.1469-185X.2010.00164.x>
- Tziritis E, Pisinaras V, Panagopoulos A, Arampatzis G (2021) RIVA: a new proposed method for assessing intrinsic groundwater vulnerability. *Environ Sci Pollut Res* 28:7043–7067. <https://doi.org/10.1007/s11356-020-10872-3>
- Yin L, Zhang E, Wang X et al (2013) A GIS-based DRASTIC model for assessing groundwater vulnerability in the Ordos Plateau, China. *Environ Earth Sci* 69:171–185. <https://doi.org/10.1007/s12665-012-1945-z>
- Yu D, Shi P, Liu Y, Xun B (2013) Detecting land use-water quality relationships from the viewpoint of ecological restoration in an urban area. *Ecol Eng* 53:205–216. <https://doi.org/10.1016/j.ecoleng.2012.12.045>

Zghibi A, Merzougui A, Chenini I et al (2016) Groundwater vulnerability analysis of Tunisian coastal aquifer: an application of DRASTIC index method in GIS environment. *Groundw Sustainable Dev* 2–3:169–181. <https://doi.org/10.1016/j.gsd.2016.10.001>

Publisher's note Springer Nature remains neutral with regard to jurisdictional claims in published maps and institutional affiliations.

Springer Nature or its licensor (e.g. a society or other partner) holds exclusive rights to this article under a publishing agreement with the author(s) or other rightsholder(s); author self-archiving of the accepted manuscript version of this article is solely governed by the terms of such publishing agreement and applicable law.